HHS Public Access

Author manuscript

J Immunol. Author manuscript; available in PMC 2022 October 01.

Published in final edited form as:

J Immunol. 2021 October 01; 207(7): 1785–1797. doi:10.4049/jimmunol.2100070.

Integrin CD11b negatively regulates B cell receptor signaling to shape humoral response during immunization and autoimmunity

Mingqian Zhou[#*,†], **Paul Dascani**[#‡], **Chuanlin Ding**[#*], **Justin T. Kos**[§], **David Tieri**[§], **Xiaoying Lin**[*,†], **Dawn Caster**[¶], **David Powell**[¶], **Chengping Wen**[†], **Corey T. Watson**[§], **Jun Yan**[*,‡]

[*]Division of Immunotherapy, The Hiram C. Polk, Jr., MD Department of Surgery, Immuno-Oncology Program, James Graham Brown Cancer Center, University of Louisville School of Medicine, Louisville, KY, USA

[†]College of Basic Medical Sciences, Zhejiang Chinese Medical University, Hangzhou, Zhejiang, China

[‡]Department of Microbiology and Immunology, University of Louisville School of Medicine, Louisville, KY, USA

[§]Department of Biochemistry and Molecular Genetics, University of Louisville, Louisville, KY, USA

[¶]Department of Medicine, University of Louisville, Louisville, KY, USA

[#] These authors contributed equally to this work.

Abstract

Our previous work has revealed the ability of CD11b to regulate B cell receptor (BCR) signaling and control autoimmune disease in mice. However, how CD11b regulates the immune response under normal conditions remains unknown. Through the use of a CD11b knockout model on a non-autoimmune background, we demonstrated that CD11b-deficient mice have an elevated antigen-specific humoral response upon immunization. Deletion of CD11b resulted in elevated low-affinity and high-affinity IgG antibody, and increases in antigen-specific germinal center (GC) B cells and plasma cells (PCs). Examination of BCR signaling in CD11b-deficient mice revealed defects in association of negative regulators pLyn and CD22 with the BCR while increases in colocations between positive regulator pSyk and BCR following stimulation. Using a CD11b-reporter mouse model, we identified multiple novel CD11b-expressing B cell subsets that are dynamically altered during immunization. Subsequent experiments using a tissue-specific CD11b deletion model revealed this effect to be B cell intrinsic, and not altered by myeloid cell CD11b expression. Importantly, CD11b expression on PCs also impacts on BCR repertoire selection and diversity in autoimmunity. These studies describe a novel role for CD11b in regulation of the healthy humoral response and autoimmunity and reveal previously unknown populations of CD11b expressing B cell subsets, suggesting a complex function for CD11b in B cells during development and activation.

Correspondence: Jun Yan, M.D., Ph.D, Division of Immunotherapy, The Hiram C. Polk, Jr., MD Department of Surgery, Immuno-Oncology Program, James Graham Brown Cancer Center, University of Louisville School of Medicine. Tel: 502 852-3628, Fax: 502 852-2123, jun.yan@louisville.edu.

Introduction

B cells are mediators of humoral immunity and can secrete antibodies which are able to bind their cognate antigens at sites distal from the B cell itself (1–3). Antibody production by B cells is a tightly regulated process. There are several mechanisms that exist to keep B cell activation in check, such as negative selection/deletion, induction of anergy, and re-editing of the B cell receptor (BCR) (4). The BCR signaling cascade is one of the major mechanisms for controlling B cell activation. The Src-family kinases LYN, BLK, and CSK serve as BCR inhibitory signals. LYN enacts inhibition by recruitment and activation of inhibitory surface receptors FcγR2B and CD22 (5). The cytoplasmic tail domains of molecules then recruit and activate Src homology domain containing inositol polyphosphate 5-phosphotase 1(SHIP-1) and SH-2-containing protein tyrosine phosphatase 1 (SHP-1) which inactive phosphorylation activation signals downstream of the BCR including PIP3 and Syk, thereby reduce the strength of the B cell activation signal (6–8). These events also determine the magnitude and longevity of the resulting humoral response (9). Proper control of these signals is crucial to maintain a healthy level of antibody response that otherwise can lead to autoimmune or immunodeficient disease if regulation is overactive or deficient, respectively (10, 11).

CD11b, the 165-kDa ITGAM, non-covalently associates with CD18 to form αMβ2, also known as macrophage-1 antigen (Mac-1) or CR3. CR3/Mac-1 is a type I membrane glycoprotein and is one of the four members of the leucocyte-restricted β2-integrin family (12–15). CD11b is conventionally considered a myeloid cell marker. However, the association of CD11b/ITGAM mutation with systemic lupus erythematosus (SLE), a disease mainly driven by T and B cell autoimmunity, suggests a potential function in lymphocytes as well. One early study found that CD11b is expressed more on $CD27^{+}IgD^{-}$ memory B cells than other peripheral B cell populations. These cells were demonstrated to migrate *in vitro* more effectively than $CD11b^{-}$ subsets, suggesting a role in homing ability for memory B cells (16). A small subset of B1 B cells, roughly 10%, expresses CD11b. These cells were found to specialize in stimulation and expansion of $CD4^{+}$ T cells and produced far less IgM than the majority $CD11b^{-}$ subset (17). A CD11b expressing population of plasma cells (PCs) has also been described. These intestinally located PCs reside in the Peyer's patch, and produce higher amounts of IgA antibody than $CD11b^{-}$ cells (18). Our previous study demonstrated that CD11b acts as a negative regulator of BCR-mediated autoreactive B cell activation/tolerance (19). However, the autoimmune setting is highly irregular. Alterations to homeostasis and bias of an autoimmune genetic background can skew the normal function of this regulatory factor. How CD11b regulates the immune response under normal conditions remains unknown.

In the current study, we examined the role of CD11b on B cell activation and antibody production in a normal, non-autoimmune setting. We also explored whether CD11b regulates BCR repertoire and diversity using CD11b reporter mice. Our data suggest that CD11b critically regulates humoral response during immunization in non-autoimmune background. Through the use of a CD11b reporter, we reveal a dynamic expression of CD11b on various B cell subsets between naïve and immune conditions. In addition, CD11b expression on PCs plays a critical role in BCR repertoire selection and diversity during

autoimmunity. These data describe a novel role for CD11b in regulating a healthy humoral response and suggest a function in controlling BCR signaling and repertoire selection at multiple stages of B cell development in health and autoimmunity.

Materials and Methods

Mice

Ig transgenic mice expressing the Vh of an anti-NP (4-hydroxy-3-nitrophenylacetyl) Ab have been fully backcrossed onto C57Bl/6 background as described previously (20). CD11b-deficient (CD11b KO) mice were purchased from the Jackson Laboratory (Bar Harbor, ME, USA) and interbred with NP Tg mice to generate NP CD11b KO mice. For the comparison experiments, NP WT and NP CD11b KO mice on a C57BL/6 background were bred in the same animal facility. CD11b-FRT reporter mice and CD11b flox/flox ($CD11b^{fl/fl}$) mice were generated by Biocytogen (Wakefield, MA) and both strains were on C57Bl/6 background. To generate myeloid cell or B cell-specific CD11b-deleted mice, LysM-Cre mice or CD19-Cre mice (Jackson Laboratory) were bred with $CD11b^{fl/fl}$ mice to generate myeloid cell or B cell specific conditional knockout mice ($CD11b^{fl/fl}LysM^{Cre/+}$ and $CD11b^{fl/fl}CD19^{Cre/+}$), respectively. Lupus-prone CD11b reporter ABIN1-FRT mice were generated by interbreeding CD11b FRT mice with ABIN1[D485N] inactive knock-in mice. The ABIN1[D485] mouse model was a gift from Dr. Philip Cohen (University of Dundee, Dundee, Scotland). Generation and characterization of lupus phenotypes in ABIN1[D485N] mice were previously described (21). All animals were maintained under specific pathogen-free conditions and handled in accordance with the protocols approved by the Institutional Animal Care and Use Committee of the University of Louisville.

Reagents

Fluorochrome-labeled mAbs against NK1.1, Gr-1, CD3, CD19, CD11b, CD22, CD23, CD21/35, IgD, CD38, CD80, CD43, IgM, B220, GL7, CD138, anti-rabbit IgG and viability detection Ab were purchased from BioLegend (San Diego, CA). NP-CGG, NP-PE, NP_{23}-BSA and NP_2-BSA were purchased from Biosearch Technologies (Petaluma, CA). Abs against Phospho-Zap-70/Syk, phospho-Lyn, and SHP-1 were obtained from Cell Signaling Technology Inc (Beverly, MA). Anti-mouse IgM-HRP and IgG-HRP were purchased from Southern Biotech (Birmingham, AL).

In vivo immunization and Antibody detection

For Th1 type immunization, NP WT and NP CD11b KO mice were immunized by subcutaneous injection (s.c.) with a solution of 50 μg of NP-CGG in complete Freund's adjuvant (CFA) at a 1:1 ratio. After 14 days, mice were boost immunized with 50 μg of NP-CGG in incomplete Freund's adjuvant (IFA) at a 1:1 ratio. Sera were collected before and at day 21 post-immunization. Anti-NP Ab was measured using parallel ELISAs in which wells were coated with 1 μg of NP_{23}-BSA or NP_2-BSA to detect low-affinity or high affinity Abs, respectively. Similarly, CD11b control or cKO mice were immunized by s.c. injection with 100 μg of OVA in CFA at a 1:1 ratio and boosted with 100 μg of OVA in IFA after 14 days. Sera were collected before and at day 21 post-immunization. Anti-OVA Ab titers were measured via ELISA using a 96-well plate coated with 1 μg of OVA. FRT

mice were immunized by s.c. injection with 100 μg of OVA or with the same volume of PBS in CFA at a 1:1 ratio and boosted with 100 μg of OVA in IFA after 14 days. Sera were collected before and at day 21 post-immunization. Anti-OVA Ab titers were measured via ELISA using a 96-well plate coated with 1 μg of OVA. The OD value read at 450 nm was used to determine the overall affinity. For Th2-type immunization, NP WT or NP CD11b KO mice were immunized via intraperitoneal (i.p.) injection of 50μg $NP_{20–29}$-CGG in Alum adjuvant at a 1:1 ratio. CD11b FRT Reporter mice were immunized via intraperitoneal (i.p.) injection of 100μg OVA peptide in Alum adjuvant at a 1:1 ratio. Sera was collected before and at given time points after immunization. Anti-NP and anti-OVA titers were measured via ELISA using a 96-well plate coated with 1 μg of NP_{22}-BSA or OVA and a standard ELISAMAX kit (Biolegend).

Flow cytometry and cell sorting

Single-cell suspensions were blocked in the presence of anti-CD16/CD32 at 4 °C for 15 min and stained on ice with the appropriate antibodies in PBS buffer. The samples were acquired using BD FACSCanto cytometer (BD Bioscience, San Jose, CA) and analyzed using FlowJo software (Tree Star, Ashland, OR). Sorting was performed using FACSAria III (BD Biosciences) or MoFlo XDP (Beckman Coulter). Cell purity was confirmed at greater than 90% via flow cytometry.

Co-localization analysis

Cells were pre-warmed in a 37 °C incubator for 2 hours and stimulated for 10 or 30 min at 37 °C with FITC-labelled anti-IgM $F(ab')_2$ (Jackson ImmunoResearch Laboratories, Inc). Both stimulated and unstimulated cells were fixed with 1.5% paraformaldehyde. Cell were then permeabilized using permeability buffer and intracellular stained with antibodies against SHP-1, CD22, CD11b, Phospho-Zap-70/Syk and phospho-Lyn in staining buffer at 4°C overnight. Alexa Fluor® 647 Donkey anti-rabbit IgG was used as secondary antibody and incubated with cells in the dark at RT for 30 min. The samples were acquired using the Amnis ImageStream system (Amnis Corporation) and analyzed using IDEAS analysis software (Amnis Corporation). The degree of co-localization was analyzed using the similarity feature.

Immunofluorescence staining

Draining LNs from OVA/CFA/IFA immunized control and CD19-cre;$CD11b^{fl/fl}$ cKO mice were embedded in OCT medium (Tissue-Tek OCT compound 4583; SAKURA) by using a dry ice-cooled 2-methylbutane (Sigma-Aldrich) bath. Cryosections (7 μm) were fixed in −20°C acetone for 20 min and air-dried at room temperature. Sections were blocked with 20% FBS in PBS for 1 hour at RT and then were stained with the following Abs at 4°C overnight: FITC-B220, PE-GL7 and APC-CD3 (BioLegend) at 1:100 dilution. After three washes with PBS, slides were mounted with Fluoro-Gel (Electron Microscopy Sciences). Images were acquired at 10× magnification using Nikon Confocal Microscope (Nikon).

BCR repertoire sequencing

Sorted CD11b positive and negative plasma cells (PCs) from CD11b reporter ABIN1 mice (4 months old; n=4) were frozen in TRIzol (Life Technologies) for RNA extraction. IgG 5'RACE expressed antibody repertoire libraries were constructed using the SMARTer Mouse BCR Profiling Kit (Takara Bio, Cat. No. 634422; Mountain View, CA, USA) following the manufacturer's instructions, with 500 ng of RNA input per library. The quality and size of each IgG library was assessed using the Agilent 2100 Bioanalyzer High Sensitivity DNA Assay Kit (Agilent, Cat. No. 5067-4626). Libraries were then pooled to 10 nM and sequenced on the Illumina MiSeq platform using the 600-cycle MiSeq Reagent Kit v3 (2×300 bp, paired-end; Illumina, Cat. No. MS-102-3003).

Antibody repertoire sequencing data processing and analysis was carried out using R packages within the Immcantation Portal. Following sample demuxing, initially processing was conducted using the Presto software package (22). Briefly, reads were trimmed to Q=20, and only reads in which the IgG primer could be identified were retained. Read mate-pairs were assembled using pairSeq and assemblePairs functions, attempting de novo assembly first, and then using blastn guided assembly if there was insufficient bp overlap between reads. A maximum overlap error rate of 0.1 between paired reads was allowed, and assembled reads <400 bp were discarded. Duplicate sequences within each library were collapsed, maintaining sequences represented by >1 read. Immunoglobulin heavy chain variable (IGHV), diversity (IGHD), and joining (IGHJ) gene assignments were determined using IgBlast (23). The germline database used included C57BL/6 germline sequences available in the ImMunoGeneTics Information System (IMGT) database (24), sequence for the gene IGHV1–2 was manually added. Clones were defined across CD11b negative and positive IgG repertoires from each animal using Change-O (25), based on IGHV/J gene assignments and junction sequence similarity (Hamming distance = 0.15). Clonal abundance curves for each IgG repertoire were estimated using the Alakazam package (26), with 200 bootstrap realizations, based on methods described in (27, 28). Repertoire diversity curves were estimated for each repertoire using the alphaDiversity function, with 200 bootstrap realizations. A one-sided paired T-test was used to assess differences in the Simpson's index ($p<0.05$). Evidence for selection on IGHV sequences within each repertoire and animal were assessed using baseline and testBaseline functions within the shazam package (29). The RDI (repertoire dissimilarity index) (30) was estimated within each cell subset using the calcRDI function. RDI values were compared between cell types using a one-way ANOVA. The sequence data have been deposited in the Sequence Read Archive (SRA) BioProject ID PRJNA706399.

Statistical analysis

Data are shown as mean ± SEM unless otherwise indicated. Statistical differences were analyzed by using a two-tailed unpaired Student's t-test. Differences were considered significant at the level $p< 0.05$. Statistical analysis was performed with GraphPad Prism software.

Results

CD11b-deficient mice exhibit enhanced antibody production and germinal center (GC) B cell response upon antigen (Ag) immunization

To examine the effect of CD11b deficiency on B activation and antibody production in normal background mice, we crossed global CD11b KO mice with NP immunoglobulin (Ig) transgenic mice. These mice carry a pre-recombined BCR heavy chain variable locus that has affinity for the hapten NP (4-hydroxy-3-nitrophenylacetyl), allowing for a greater scale response following immunization. In addition, this system allows NP-specific B cells to be identified. CD11b deficiency in KO B cells was confirmed by Western blot analysis (Figure S1A). NP WT and NP CD11b KO mice were immunized with 50 μg of NP-CGG (NP-chicken gamma globulin conjugate) following CFA-IFA protocol (Th1-type). Sera were collected before and at day 21 post-immunization and anti-NP Ab response (high affinity and low affinity IgG levels) was measured by ELISA. Compared to pre-immunization, both WT and KO mice showed the increased anti-NP IgG levels at day 21 postimmunization (Figure 1A). In addition, the titers of both low-affinity and high-affinity anti-NP IgG in KO mice were higher than those in WT mice, indicating a dysregulation of the B cell response to Ag immunization in the absence of CD11b. We then examined the frequency of total plasma cells (PCs, $B220^{dim}CD138^{+}$), plasmablasts ($B220^{hi}CD138^{+}$) and GC B cells ($B220^{+}GL7^{hi}$) as well as frequency of NP-specific PCs, plasmablast, and GC B cells in this model. The gating strategy was shown in Figure S1C. In the spleen, the frequency of PCs, plasmablasts and GC B cells was comparable in both NP CD11b KO and WT mice (Figure 1B). However, when examining the NP-specific cell population, we found the frequency of NP^{+} PCs in CD11b KO mice was higher than that in WT mice, although NP^{+} plasmablasts and NP^{+} GC B cells were comparable between WT and CD11b KO mice (Figure 1C). Unlike the spleen, CD11b KO mice had increased total plasmablasts and GC B cells in draining lymph nodes (LN) comparing to WT mice (Figure 1D). In addition, the NP-specific subsets had an even stronger phenotype in draining LN. The frequencies of NP^{+} PCs, NP^{+} plasmablasts and NP^{+} GC B cells in CD11b KO mice were significantly higher than those in WT mice (Figure 1E).

We next examined whether global CD11b deficiency has similar effect on Th2-type immunization. To this end, WT or CD11b KO NP Tg mice were immunized with $NP_{20–29}$-CGG in Alum adjuvant. At day 14, anti-NP IgG level was elevated in CD11b KO mice compared to WT controls. Baseline IgM antibody was also increased in these mice (Figure 2A). Although we did not observe any significant change in total GC B cells, NP-specific GC B cells were significantly increased in CD11b KO mice (Figure 2B). Total PCs were also increased in addition to the NP-specific subset (Figure 2C). Increases in both of these populations suggest CD11b negative regulation is able to limit the high affinity antibody response, though there is a bystander effect at PC stage. Taken together, these data demonstrate an Ag-restricted negative-regulatory role for CD11b on the maintenance of PC and GC B populations, which impacts the magnitude of the antibody response.

The loss of CD11b promotes BCR activation signal and reduces inhibitory signal

Ag-driven BCR signaling plays a critical role in the initiation of B cell activation and differentiation into antibody-secreting PCs (31). Previous studies have shown that the BCR

signaling is regulated by the availability of Ags as well as co-stimulatory and co-inhibitory receptors such as CD79, CD22, CD45, and Galectin-9 (32) through the activation of the tyrosine kinase Syk and Lyn or SHP-1 (33, 34). Activation of Syk is associated with BCR stimulatory receptor while Lyn activation and SHP-1 negatively regulate BCR signaling. To determine whether CD11b deficiency directly regulates BCR signaling as we previously demonstrated in autoreactive B cells (19), B cells from draining LNs of immunized WT or CD11b KO NP Tg mice were stimulated with or without FITC-labeled anti-IgM $F(ab')_2$ fragment to mimic BCR crosslinking. Cells were then analyzed using ImageStream. Percent of co-localization was determined by the similarity score. As shown in Figure 3A, unstimulated CD11b KO B cells exhibited more BCR-pSyk co-localizations than WT B cells. Upon BCR crosslinking, more BCR-pSyk colocalization was noticed at 30 min. In addition, there was more BCR-pSyk co-localization in CD11b KO B cells compared to WT B cells. In contrast, WT B cells exhibited more BCR–pLyn co-localizations compared to B cells without CD11b (Figure 3B). In addition, with the BCR stimulation, CD11b KO B cells showed a blunted response in BCR-pLyn colocalization. BCR ligation resulted in the association of pSyk, pLyn, and SHP-1 from BCR in both groups. There was no significant difference in the colocalization of BCR-SHP-1 between the two groups (Figure 3C). The differential colocalizations of pSyk and pLyn with BCR in B cells from immunized NP WT mice versus NP CD11b KO mice suggest that CD11b serves as a negative regulator in BCR signaling, which could inhibit activation signals, such as pSyk, and promote inhibitory signals, such as pLyn.

To further confirm these findings, B cells were purified from draining LNs of immunized NP Tg mice and then stimulated with FITC-labeled anti-IgM $F(ab')_2$ fragment. These B cells were also stained with CD11b antibody to differentiate $CD11b^+$ from $CD11b^-$ B cells. As shown in Figure S2A, unstimulated $CD11b^-$ B cells exhibited more BCR-pSyk co-localizations than $CD11b^+$ B cells. Upon BCR crosslinking, there was more BCR-pSyk co-localization in $CD11b^-$ B cells compared to $CD11b^+$ B cells. In contrast, $CD11b^+$ B cells exhibited more BCR–pLyn co-localizations compared to CD11b- B cells with the BCR stimulation (Figure S2B). These data are largely consistent with CD11b WT and KO B cells shown in Figure 3. We also examined co-localization between BCR and negative regulator CD22. We found that $CD11b^-$ B cells showed decreased BCR-CD22 colocalization upon BCR crosslinking (Figure S2C). Collectively, these data suggest that CD11b serves as a checkpoint molecule in regulating BCR signaling.

CD11b expression levels on different B Cell compartment in a steady state and upon immunization

Our previous study has showed CD11b expression on B cells (19). However, expression of CD11b at each stage of B cell development is not well characterized. In order to examine this, we generated a CD11b-reporter mouse model which adds a GFP tag to the CD11b promoter site (Figure S3A). We first sought to investigate any changes in CD11b expression under immune conditions compared to the naïve state and a Th2 type immunization was used. Beginning at the early stages of development, we examined the pre-pro B (fraction A), pro B (fraction B), pre B (fraction C), and immature B cell (fraction D) populations in the bone marrow (BM). Expression was greatest at the earliest pre-pro B cell stage, and

increased even further after immunization (Figure S3B, C). In the intermediate pro B and pre B stages, the CD11b expression was minimal, averaging less than even 1% of the total population. By the immature B cell phase, expression elevated slightly, and was once again increased in the immune setting (Figure S3C). As a whole, the developmental stages of B cells have minimal levels of CD11b expression compared to other subsets.

In the peripheral lymphoid organs, we revealed CD11b expression in the follicular (FO) and marginal zone (MZ) B cells of the spleen. The FO B compartment revealed a low but very well-defined population of CD11b expressing cells (Figure 4A). Interestingly, expression decreased by nearly half after immunization. The MZ $CD11b^{+}$ subset was larger, and also showed a similar decrease in immunized mice. Also within the spleen, we examined GC B cells to reveal an average of 2% of naïve GC B cells express CD11b which decreased by nearly half following immunization (Figure S3D). Post-GC long lived memory B cells reside in the spleen as well. CD11b expression in these cells increased dramatically after Th2 immunization (Figure 4B). Among the B cell subsets examined, the PCs carry the most consistently high amounts of CD11b expression. An average of 12% of splenic-resident short-lived plasma cells express CD11b in the naïve state, which decreased after immunization (Figure 4C). Surprisingly, the opposite effect was observed in BM resident long-lived PCs. Here, CD11b expression averaged at roughly 8% increased after immunization (Figure 4D). The opposing shift in expression under immunization conditions indicates a differential role for CD11b in these two closely related but distinct populations. We also used Th1-type immunization and observed similar decreased CD11b expression in PC and GC B cells upon immunization (Figure 4E). The varying changes in expression across all of these B cell subsets outlines a complex and dynamic role for CD11b regulation.

Loss of CD11b on myeloid cells does not impact the antibody response

CD11b is conventionally considered as a marker for myeloid cells. Although in our studies, we used dump gating strategy to gate out myeloid cells, T cells, and NK cells, it is possible that some myeloid cells remain in the gated cells. To further investigate the role of CD11b on different subsets of cells, we generated $CD11b^{fl/fl}$ mice using CRISPR/Cas9 technology and then bred these mice with LysM Cre mice to establish a CD11b conditional knockout model that specifically depletes CD11b expression in myeloid cells. We found a roughly 75% reduction of CD11b expression on myeloid cells (Figure 5A). These mice were immunized with OVA using CFA/IFA protocol (Th1 type). Unlike our previous results, no changes were observed in the IgG antibody response between the control and the CD11b cKO mice (Figure 5B). The frequencies of PCs and GC B cells in the spleen (data not shown) or draining LN were unaffected (Figure 5C). We further immunized these mice using Th2 type immunization. Both mouse strains produced larger amounts of anti-OVA IgG, however, no difference was observed between the two groups (Figure 5D). In addition, the frequency of PCs and GC B cells was comparable in the spleen of both mouse strains (Figure 5E). These results suggest that CD11b deficiency on myeloid cells does not alter the humoral immune response.

B cell intrinsic CD11b regulates the antibody response

To better elucidate the cell-specific importance of CD11b in this phenotype, we generated a CD19-cre;CD11b$^{fl/fl}$ conditional knockout (cKO) model. CD11b depletion efficiency in B cells were evaluated with Western blot analysis. B cells from CD11b cKO mice expressed substantially lower CD11b compared to control B cells (Figure S1B). These mice were then immunized with 100 μg of OVA in CFA/IFA protocol. Twenty-one days after immunization, anti-OVA IgG antibodies increased significantly in CD19-cre;CD11b$^{fl/fl}$ cKO mice compared to those from control mice (Figure 6A), mimicking the phenotype of global CD11b knockouts. We also performed IgG subtype analysis. IgG2b levels were significantly increased in the cKO mice compared to control mice; IgG1 levels were comparable between the two groups. The frequency of GC B cells and PCs was also examined in the spleen and LN. Neither GC B cells nor PCs were altered in the spleen (data not shown). However, compared with CD11b$^{fl/fl}$ control mice, CD19-Cre;CD11b$^{fl/fl}$ cKO mice had a significant increase of PCs and GC B cells in the draining LN (Figure 6B). The increased GC formation in the draining LNs was also revealed in CD19-Cre;CD11b$^{fl/fl}$ cKO mice assessed by confocal microscopy (Figure 6C). Similarly, elevated antibody production was also seen in Th2 type immunization in cKO mice compared to control mice (Figure 6D). These results further demonstrate the importance of CD11b expression on B cells in regulating the humoral immune response in a non-autoimmune setting.

CD11b expression on plasma cells impacts on autoreactive B cell repertoire

As we discovered high expression levels of CD11b on PCs, we next examined whether CD11b expression impacted B cell receptor repertoire selection in addition to regulating the overall antibody response. Since autoreactive B cells can spontaneously secrete autoantibodies, we then backcrossed CD11b reporter mice onto ABIN1[D485N] lupus-prone mice. A20-binding inhibitor of NF-kB (ABIN1) is a ubiquitin-binding protein that has been identified as a SLE susceptibility locus in a genome-wide studies (35, 36). These mice develop autoAbs including anti-dsDNA starting at 3-months of age and are not subject to the bias of the Fas^{lpr} model whose lack of Fas-FasL interaction heavily skews selection of the B cell population (21). We used 4-month old ABIN1[D485N] mice and gated on the PCs and found that CD11b was expressed on 20%−30% of PCs (Figure 7A). To examine whether CD11b influenced the B cell repertoire, we sorted CD11b positive and negative PCs and performed expressed antibody repertoire sequencing. As shown in Figure 7B and 7C, within mice the IgG repertoires of CD11b positive PCs were less diverse than CD11b negative PCs, and tended to be dominated by more highly abundant clones (Figure S4A). This suggests that loss of CD11b on autoreactive B cells may limit the specific selection of particular antibody clones, leading to a more unadulterated and diverse repertoire. This was also suggested via the analysis of somatic hypermutation patterns, as we observed evidence of positive selection in IgG IGHV complementary determining regions (CDRs) among sequences of clonal lineages in CD11b positive cell repertoires (Figure 7D). Density plots from each mouse were shown in the Figure S4B. Finally, examination of global patterns in IGHV gene usage between samples of each group using the repertoire dissimilarity index (RDI) also revealed that the repertoires of CD11b negative PCs were more similar to each other than were repertoires among CD11b positive PCs (Figure 7E; $P = 0.00003$, one-

way ANOVA). Taken together, these data strongly suggest that CD11b critically regulates antibody repertoire diversity, abundance and potentially autoreactivity.

Discussion

In the present work, we utilized a non-autoimmune setting to observe the effect of CD11b on the healthy humoral response, and identify novel and dynamic CD11b expression on B cell subsets. We observed an increased antibody response in both CD11b global KO and B cell-specific depleted mice, suggesting that this effect is not dependent on the autoimmune nature as we showed previously (19). This phenotype is also seen in both Th1- and Th2-type immunizations. The increase in both switched IgG and non-switched IgM antibody shows this regulation impacts antibody resulting from GC B cells as well as extrafollicular B cells. The “choice” between these two maturation pathways is governed by Ag recognition strength, thus implying that B cell CD11b regulation is not dependent on the intensity of BCR-Ag binding (37). However, the NP-specific sub-population of PCs and GCs was elevated in CD11b KO mice, suggesting that CD11b may have more effect on Ag-specific B cell activation and differentiation.

The BCR signaling cascade acts through and is regulated by phosphorylation-controlled proteins such as Syk, Lyn, and SHP-1. In the absence of stimulation, BCRs cluster into autoinhibitory confirmations. Our previous work demonstrated CD11b has a stabilizing effect on CD22, which maintains the inhibitory cluster state to control tonic BCR signaling (38). Binding of Ag causes dispersal of these clusters, opening up immunoreceptor tyrosine-based activation motifs (ITAMs) on the cytoplasmic portions of associated CD79 which in turn recruit downstream signals such as Lyn and Syk (39, 40). Indeed, we observed a significant increased BCR-pSyk colocalization in CD11b deficient B cells even at the basal level. In contrast, BCR-pLyn colocalization is decreased in CD11b deficient B cells upon BCR activation, demonstrating its involvement in maintaining the pLyn negative regulatory circuit on B cells. Similar to autoreactive B cells (19), we also observed less co-localization between BCR and CD22 in $CD11b^{-}$ B cells upon BCR crosslink. These observations further confirm CD11b’s function in the regulatory circuit of BCR activation. Whether it is serving a specific regulatory purpose at this stage or simply retaining its function as a permanent feature of the BCR circuit has yet to be determined.

Use of a tissue specific knockout model to eliminate B cell CD11b expression was able to replicate the increase in serum IgG and IgM seen in the global knockout mice. In addition, the frequency of PCs and GC B cells was also elevated in B cell-specific CD11b deficient mice. In contrast, usage of myeloid cell expressed lysosome-cre driven conditional knockout was unable to replicate any of the enhanced B cell response phenotypes seen in CD11b global knockout animals although previous studies showed that CD11b expressing myeloid cells are important in the priming and expansion of B cells during an alum immunization reaction (41, 42). Even CD11b expressing myeloid-derived suppressor cells (MDSCs) have been shown to enhance B cell antibody production in certain settings (43, 44). Interestingly, CD11b expressing myeloid cells were found to suppress lupus-like disease in male, but not female, NZB mice (45). Depletion of CD11b expressing neutrophils can even cause accelerated disease in both genders of these mice (46).

CD11b expressing B cell subsets have been previously identified, namely in the memory B cell, B1 B cell, and Peyer's patch resident PC subsets (16–18). Using a CD11b reporter, we were able to identify small subsets (2% or less) of CD11b expressing FO, MZ, and GC B cells which decreased even further following immunization. The relatively low frequency of these fractions suggests a tightly controlled but necessary role for CD11b in regulating a specific sub-population of cells. We also confirmed previous reports of a substantial CD11b expressing fraction of memory B cells, which increased after immunization. Here, CD11b is likely to assist in migration and tissue homing following generation as previously shown, but may also have functions in controlling activation as shown in other subsets (16). Expanding upon the CD11b expressing PCs previously identified in the Peyer's patch, we observed CD11b positive populations of both splenic and BM resident PCs. In the splenic population, which are typically short-lived PCs, CD11b expression decreased following immunization. The aforementioned CD11b expressing Peyer's patch PCs were found to proliferate and produce antibody at a higher rate than $CD11b^{-}$ cells (18). Increased CD11b expression may serve as a negative regulator to better control these hyper-responsive cells. Splenic PC CD11b could function in a similar role by tempering the response of newly formed PCs, which carry reduced expression as they complete differentiation and exit the GC. Conversely, long-lived PCs of the BM increased CD11b expression following immunization. Long-lived PCs do not activate and respond to BCR binding Ag or immune complex, but rather exist to provide persistent antibody after initial encounter with Ag (47, 48). Here, high CD11b expression may serve as an additional layer of regulation to prevent BCR signal activation of these cells and maintain a steady state of antibody production. However, the underlying mechanisms that regulate CD11b dynamic expression at different states need to be determined in the future work.

We further demonstrate that CD11b expression is also involved in BCR repertoire selection and diversity. The IgG repertoires of CD11b positive PCs were less diverse than CD11b negative PCs and were dominated by more highly abundant clones. This suggests that loss of CD11b on autoreactive B cells may lead to a lack of regulatory constraint, limiting the specific selection of particular antibody clones, leading to more diverse repertoire, consistent with our overall conclusion that CD11b is a negative regulator of BCR signaling. This also suggests that CD11b not only regulates the magnitude of antibody production but also impacts on the quality of antibody production via influence on the selection of particular antibody clones. This is important given the fact that protective antibodies are critical in eliminating pathogens while pathogenic autoantibodies promote disease pathogenesis. Understanding how CD11b regulates B cell activation and differentiation in health and disease may provide a novel target for the treatment of infectious diseases and autoimmune disorders.

Supplementary Material

Refer to Web version on PubMed Central for supplementary material.

Acknowledgments

This work was supported by the NIH R21AI124235 and AI124081. CD, DT, CTW, and JY were supported in part by NIH P20 GM135004.

Reference

1. Nimmerjahn F, and Ravetch JV. 2008. Fcgamma receptors as regulators of immune responses. Nat Rev Immunol8: 34–47. [PubMed: 18064051]
2. Pignata ML, Gudino GL, Canas MS, and Orellana L. 1999. Relationship between foliar chemical parameters measured in Melia azedarach L. and environmental conditions in urban areas. Sci Total Environ243–244: 85–96.
3. de Valliere S, Abate G, Blazevic A, Heuertz RM, and Hoft DF. 2005. Enhancement of innate and cell-mediated immunity by antimycobacterial antibodies. Infect Immun73: 6711–6720. [PubMed: 16177348]
4. Pelanda R, and Torres RM. 2012. Central B-cell tolerance: where selection begins. Cold Spring Harb Perspect Biol4: a007146. [PubMed: 22378602]
5. Tsubata T2012. Role of inhibitory BCR co-receptors in immunity. Infect Disord Drug Targets12: 181–190. [PubMed: 22394175]
6. Hua Z, Gross AJ, Lamagna C, Ramos-Hernandez N, Scapini P, Ji M, Shao H, Lowell CA, Hou B, and DeFranco AL. 2014. Requirement for MyD88 signaling in B cells and dendritic cells for germinal center anti-nuclear antibody production in Lyn-deficient mice. J Immunol192: 875–885. [PubMed: 24379120]
7. Dustin LB, Plas DR, Wong J, Hu YT, Soto C, Chan AC, and Thomas ML. 1999. Expression of dominant-negative src-homology domain 2-containing protein tyrosine phosphatase-1 results in increased Syk tyrosine kinase activity and B cell activation. J Immunol162: 2717–2724. [PubMed: 10072516]
8. Conde C, Gloire G, and Piette J. 2011. Enzymatic and non-enzymatic activities of SHIP-1 in signal transduction and cancer. Biochem Pharmacol82: 1320–1334. [PubMed: 21672530]
9. Yam-Puc JC, Zhang L, Zhang Y, and Toellner K-M. 2018. Role of B-cell receptors for B-cell development and antigen-induced differentiation. F1000Research7: 429–429. [PubMed: 30090624]
10. Königsberger S, Prodöhl J, Stegner D, Weis V, Andreas M, Stehling M, Schumacher T, Böhmer R, Thielmann I, van Eeuwijk JMM, Nieswandt B, and Kiefer F. 2012. Altered BCR signalling quality predisposes to autoimmune disease and a pre-diabetic state. The EMBO journal31: 3363–3374. [PubMed: 22728826]
11. van de Ven AA, Compeer EB, van Montfrans JM, and Boes M. 2011. B-cell defects in common variable immunodeficiency: BCR signaling, protein clustering and hardwired gene mutations. Crit Rev Immunol31: 85–98. [PubMed: 21542788]
12. Ross GD2002. Role of the lectin domain of Mac-1/CR3 (CD11b/CD18) in regulating intercellular adhesion. Immunol Res25: 219–227. [PubMed: 12018461]
13. Springer TA1994. Traffic signals for lymphocyte recirculation and leukocyte emigration: the multistep paradigm. Cell76: 301–314. [PubMed: 7507411]
14. Hogg N, and Berlin C. 1995. Structure and function of adhesion receptors in leukocyte trafficking. Immunol Today16: 327–330. [PubMed: 7576066]
15. Petty HR, and Todd RF 3rd. 1993. Receptor-receptor interactions of complement receptor type 3 in neutrophil membranes. J Leukoc Biol54: 492–494. [PubMed: 8228627]
16. Kawai K, Tsuno NH, Matsuhashi M, Kitayama J, Osada T, Yamada J, Tsuchiya T, Yoneyama S, Watanabe T, Takahashi K, and Nagawa H. 2005. CD11b-mediated migratory property of peripheral blood B cells. Journal of Allergy and Clinical Immunology116: 192–197.
17. Griffin DO, and Rothstein TL. 2011. A small CD11b(+) human B1 cell subpopulation stimulates T cells and is expanded in lupus. The Journal of Experimental Medicine208: 2591–2598. [PubMed: 22110167]
18. Kunisawa J, Gohda M, Hashimoto E, Ishikawa I, Higuchi M, Suzuki Y, Goto Y, Panea C, Ivanov II, Sumiya R, Aayam L, Wake T, Tajiri S, Kurashima Y, Shikata S, Akira S, Takeda K, and Kiyono H. 2013. Microbe-dependent CD11b(+) IgA(+) plasma cells mediate robust early-phase intestinal IgA responses in mice. Nat Commun4: 1772. [PubMed: 23612313]
19. Ding C, Ma Y, Chen X, Liu M, Cai Y, Hu X, Xiang D, Nath S, Zhang HG, Ye H, Powell D, and Yan J. 2013. Integrin CD11b negatively regulates BCR signalling to maintain autoreactive B cell tolerance. Nature communications4: 2813.

20. Yan J, Harvey BP, Gee RJ, Shlomchik MJ, and Mamula MJ. 2006. B Cells Drive Early T Cell Autoimmunity In Vivo prior to Dendritic Cell-Mediated Autoantigen Presentation. J Immunol177: 4481–4487. [PubMed: 16982884]
21. Nanda SK, Venigalla RK, Ordureau A, Patterson-Kane JC, Powell DW, Toth R, Arthur JS, and Cohen P. 2011. Polyubiquitin binding to ABIN1 is required to prevent autoimmunity. J Exp Med208: 1215–1228. [PubMed: 21606507]
22. Vander Heiden JA, Yaari G, Uduman M, Stern JN, O'Connor KC, Hafler DA, Vigneault F, and Kleinstein SH. 2014. pRESTO: a toolkit for processing high-throughput sequencing raw reads of lymphocyte receptor repertoires. Bioinformatics30: 1930–1932. [PubMed: 24618469]
23. Ye J, Ma N, Madden TL, and Ostell JM. 2013. IgBLAST: an immunoglobulin variable domain sequence analysis tool. Nucleic Acids Res41: W34–40. [PubMed: 23671333]
24. Giudicelli V, Duroux P, Ginestoux C, Folch G, Jabado-Michaloud J, Chaume D, and Lefranc MP. 2006. IMGT/LIGM-DB, the IMGT comprehensive database of immunoglobulin and T cell receptor nucleotide sequences. Nucleic Acids Res34: D781–784. [PubMed: 16381979]
25. Gupta NT, Vander Heiden JA, Uduman M, Gadala-Maria D, Yaari G, and Kleinstein SH. 2015. Change-O: a toolkit for analyzing large-scale B cell immunoglobulin repertoire sequencing data. Bioinformatics31: 3356–3358. [PubMed: 26069265]
26. Stern JN, Yaari G, Vander Heiden JA, Church G, Donahue WF, Hintzen RQ, Huttner AJ, Laman JD, Nagra RM, Nylander A, Pitt D, Ramanan S, Siddiqui BA, Vigneault F, Kleinstein SH, Hafler DA, and O'Connor KC. 2014. B cells populating the multiple sclerosis brain mature in the draining cervical lymph nodes. Sci Transl Med6: 248ra107.
27. Chao A, Hsieh TC, Chazdon RL, Colwell RK, and Gotelli NJ. 2015. Unveiling the species-rank abundance distribution by generalizing the Good-Turing sample coverage theory. Ecology96: 1189–1201. [PubMed: 26236834]
28. Chao A, et al.2014. Rarefaction and extrapolation with Hill numbers: A framework for sampling and estimation in species diversity studies. Ecol Monogr84: 45–67.
29. Yaari G, Uduman M, and Kleinstein SH. 2012. Quantifying selection in high-throughput Immunoglobulin sequencing data sets. Nucleic Acids Res40: e134. [PubMed: 22641856]
30. Bolen CR, Rubelt F, Vander Heiden JA, and Davis MM. 2017. The Repertoire Dissimilarity Index as a method to compare lymphocyte receptor repertoires. BMC Bioinformatics18: 155. [PubMed: 28264647]
31. Kwak K, Akkaya M, and Pierce SK. 2019. B cell signaling in context. Nat Immunol20: 963–969. [PubMed: 31285625]
32. Tsubata T2018. Ligand Recognition Determines the Role of Inhibitory B Cell Co-receptors in the Regulation of B Cell Homeostasis and Autoimmunity. Front Immunol9: 2276. [PubMed: 30333834]
33. Li HL, Davis W, and Pure E. 1999. Suboptimal cross-linking of antigen receptor induces Syk-dependent activation of p70S6 kinase through protein kinase C and phosphoinositol 3-kinase. J Biol Chem274: 9812–9820. [PubMed: 10092671]
34. Li HL, Davis WW, Whiteman EL, Birnbaum MJ, and Pure E. 1999. The tyrosine kinases Syk and Lyn exert opposing effects on the activation of protein kinase Akt/PKB in B lymphocytes. Proc Natl Acad Sci U S A96: 6890–6895. [PubMed: 10359809]
35. Caster DJ, Korte EA, Nanda SK, McLeish KR, Oliver RK, G'Sell RT, Sheehan RM, Freeman DW, Coventry SC, Kelly JA, Guthridge JM, James JA, Sivils KL, Alarcon-Riquelme ME, Scofield RH, Adrianto I, Gaffney PM, Stevens AM, Freedman BI, Langefeld CD, Tsao BP, Pons-Estel BA, Jacob CO, Kamen DL, Gilkeson GS, Brown EE, Alarcon GS, Edberg JC, Kimberly RP, Martin J, Merrill JT, Harley JB, Kaufman KM, Reveille JD, Anaya JM, Criswell LA, Vila LM, Petri M, Ramsey-Goldman R, Bae SC, Boackle SA, Vyse TJ, Niewold TB, Cohen P, and Powell DW. 2013. ABIN1 dysfunction as a genetic basis for lupus nephritis. J Am Soc Nephrol24: 1743–1754. [PubMed: 23970121]
36. Korte EA, Caster DJ, Barati MT, Tan M, Zheng S, Berthier CC, Brosius FC 3rd, Vieyra MB, Sheehan RM, Kosiewicz M, Wysoczynski M, Gaffney PM, Salant DJ, McLeish KR, and Powell DW. 2017. ABIN1 Determines Severity of Glomerulonephritis via Activation of Intrinsic Glomerular Inflammation. Am J Pathol187: 2799–2810. [PubMed: 28935578]

37. Paus D, Phan TG, Chan TD, Gardam S, Basten A, and Brink R. 2006. Antigen recognition strength regulates the choice between extrafollicular plasma cell and germinal center B cell differentiation. The Journal of Experimental Medicine203: 1081–1091. [PubMed: 16606676]

38. Depoil D, and Dustin ML. 2016. Agile CD22 nanoclusters run rings around fenced BCR. The EMBO journal35: 237–238. [PubMed: 26746852]

39. Buchner M, and Müschen M. 2014. Targeting the B cell receptor signaling pathway in B lymphoid malignancies. Current opinion in hematology21: 341–349. [PubMed: 24811161]

40. Fiala GJ, Kaschek D, Blumenthal B, Reth M, Timmer J, and Schamel WWA. 2013. Pre-Clustering of the B Cell Antigen Receptor Demonstrated by Mathematically Extended Electron Microscopy. Frontiers in Immunology4: 427. [PubMed: 24367367]

41. Rimaniol A-C, Gras G, Verdier F, Capel F, Grigoriev VB, Porcheray F, Sauzeat E, Fournier J-G, Clayette P, Siegrist C-A, and Dormont D. 2004. Aluminum hydroxide adjuvant induces macrophage differentiation towards a specialized antigen-presenting cell type. Vaccine22: 3127–3135. [PubMed: 15297065]

42. Jordan MB, Mills DM, Kappler J, Marrack P, and Cambier JC. 2004. Promotion of B Cell Immune Responses via an Alum-Induced Myeloid Cell Population. Science304: 1808–1810. [PubMed: 15205534]

43. Xu X, Meng Q, Erben U, Wang P, Glauben R, Kühl AA, Wu H, Ma CW, Hu M, Wang Y, Sun W, Jia J, Wu X, Chen W, Siegmund B, and Qin Z. 2017. Myeloid-derived suppressor cells promote B-cell production of IgA in a TNFR2-dependent manner. Cellular and Molecular Immunology14: 597–606. [PubMed: 27133471]

44. Lelis FJN, Jaufmann J, Singh A, Fromm K, Teschner AC, Pöschel S, Schäfer I, Beer-Hammer S, Rieber N, and Hartl D. 2017. Myeloid-derived suppressor cells modulate B-cell responses. Immunology Letters188: 108–115. [PubMed: 28687234]

45. Trigunaite A, Khan A, Der E, Song A, Varikuti S, and J∅rgensen TN. 2013. Gr-1highCD11b+ Cells Suppress B Cell Differentiation and Lupus-like Disease in Lupus-Prone Male Mice. Arthritis & Rheumatism65: 2392–2402. [PubMed: 23754362]

46. Bird AK, Chang M, Barnard J, Goldman BI, Meednu N, Rangel-Moreno J, and Anolik JH. 2017. Neutrophils Slow Disease Progression in Murine Lupus via Modulation of Autoreactive Germinal Centers. The Journal of Immunology199: 458–466. [PubMed: 28584005]

47. Manz RA, Lohning M, Cassese G, Thiel A, and Radbruch A. 1998. Survival of long-lived plasma cells is independent of antigen. Int Immunol10: 1703–1711. [PubMed: 9846699]

48. Hoyer BF, Moser K, Hauser AE, Peddinghaus A, Voigt C, Eilat D, Radbruch A, Hiepe F, and Manz RA. 2004. Short-lived Plasmablasts and Long-lived Plasma Cells Contribute to Chronic Humoral Autoimmunity in NZB/W Mice. The Journal of Experimental Medicine199: 1577–1584. [PubMed: 15173206]

Key points:

1. CD11b deficiency on B cells results in an enhanced antibody response
2. CD11b regulates BCR signaling through the Syk-Lyn-CD22 circuit
3. CD11b expression on plasma cells impacts on BCR repertoire selection and diversity

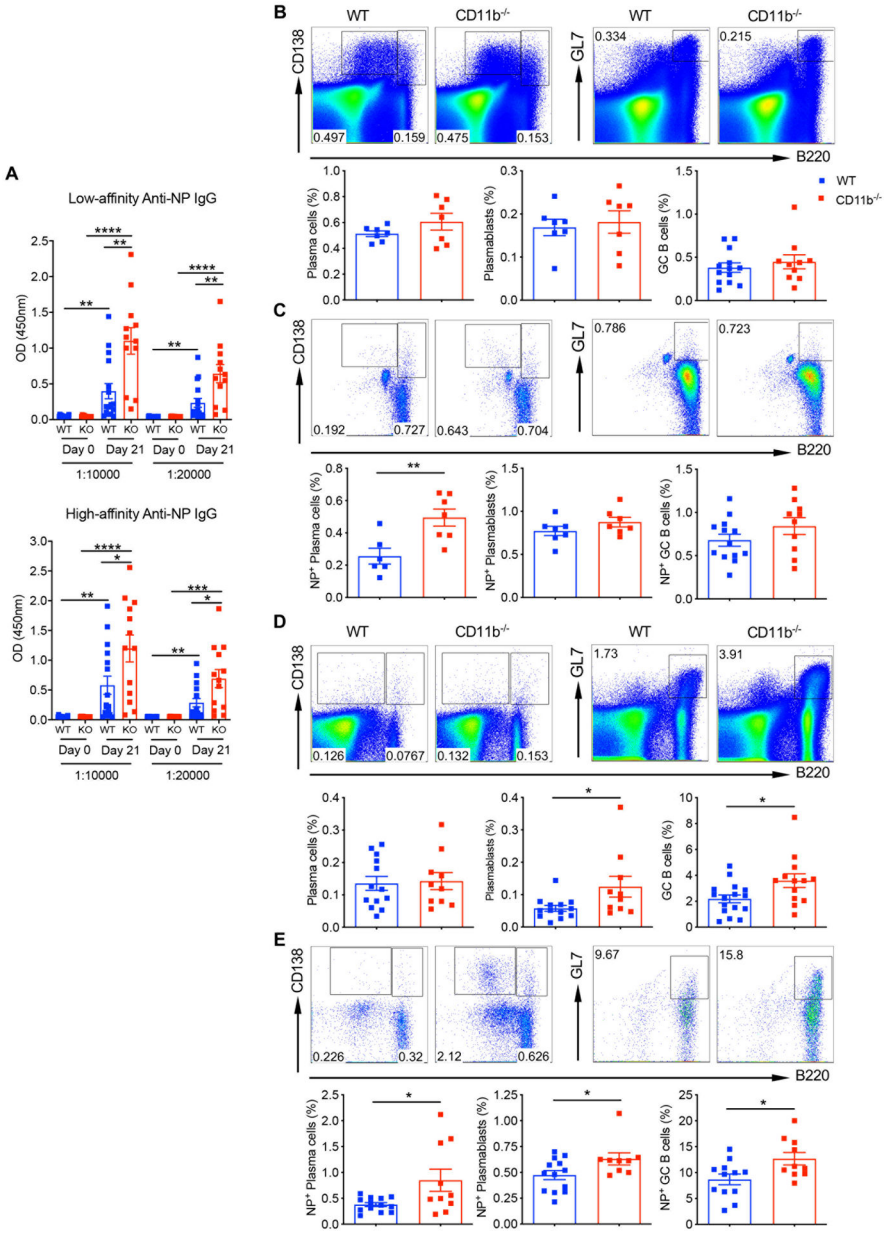

Figure 1. CD11b-deficient mice have enhanced antibody production and higher number of Ag-specific PCs and GC B cells following immunization.

NP WT and NP CD11b KO mice were immunized s.c. with a solution of 50 μg of NP-CGG emulsified in CFA at a 1:1 ratio. After 14 days, mice were boost immunized with 50 μg of NP-CGG in IFA at a 1:1 ratio. (A) Sera were collected before and at day 21 postimmunization. Anti-NP IgG levels with different affinity were measured by ELISA with NP_2-BSA (high affinity) and NP_{23}-BSA (low affinity)-coated plates. Optical density (OD) value was measured at 450nm. Spleen (B, C) and draining LN (D, E) were harvested on day 21 post-immunization. FACS analysis of total (B, D) and NP-specific (gated on NP^+ population, C, E) PCs, plasmablasts, and GC B cells are shown. Representative dot plots and summarized data are shown. Data are shown as means ± s.e.m. *P<0.05; **P<0.01;

***P<0.001; ****p < 0.0001 (unpaired two-tailed Student's t-test). Each point represents an individual mouse.

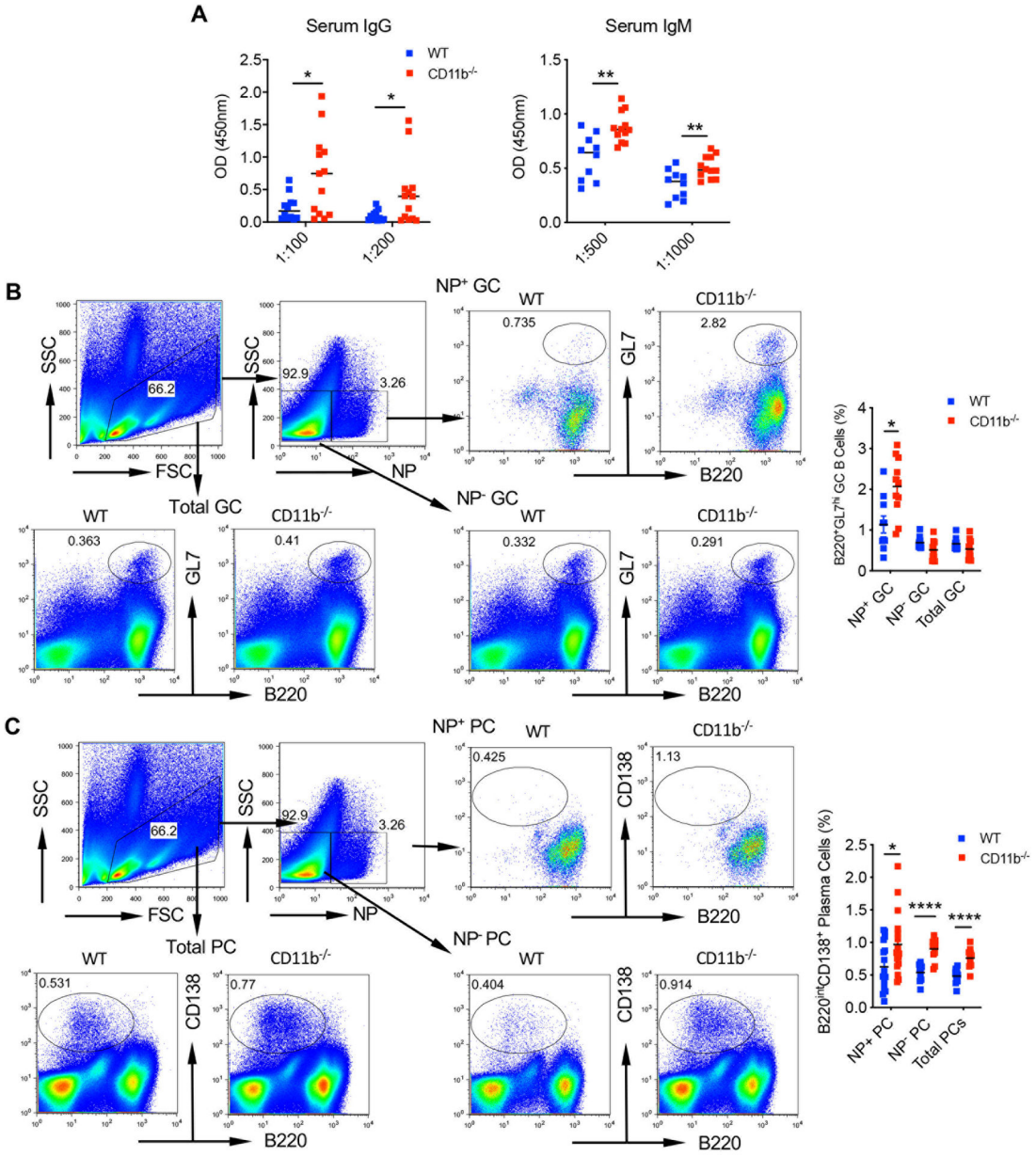

Figure 2. Global CD11b deficiency alters the Th2 humoral response.

NP WT and NP CD11b KO mice were immunized with 50μg of NP-CGG suspended in Alum via i.p. injection. (A) Serum was collected on day 14 post-immunization. Anti-NP IgG and IgM antibody was measured via ELISA in plates coated with 1μg/well of NP-BSA. OD was measured at 450nm. Data are means±s.e.m. (B, C) FACS analysis of splenic GC B cells (B) and PCs (C) from day 14 post-immunization mice. Representative dot plots and summarized results are shown. *P<0.05; **P<0.01; ****P<0.0001 (unpaired two-tailed Student's t-test).

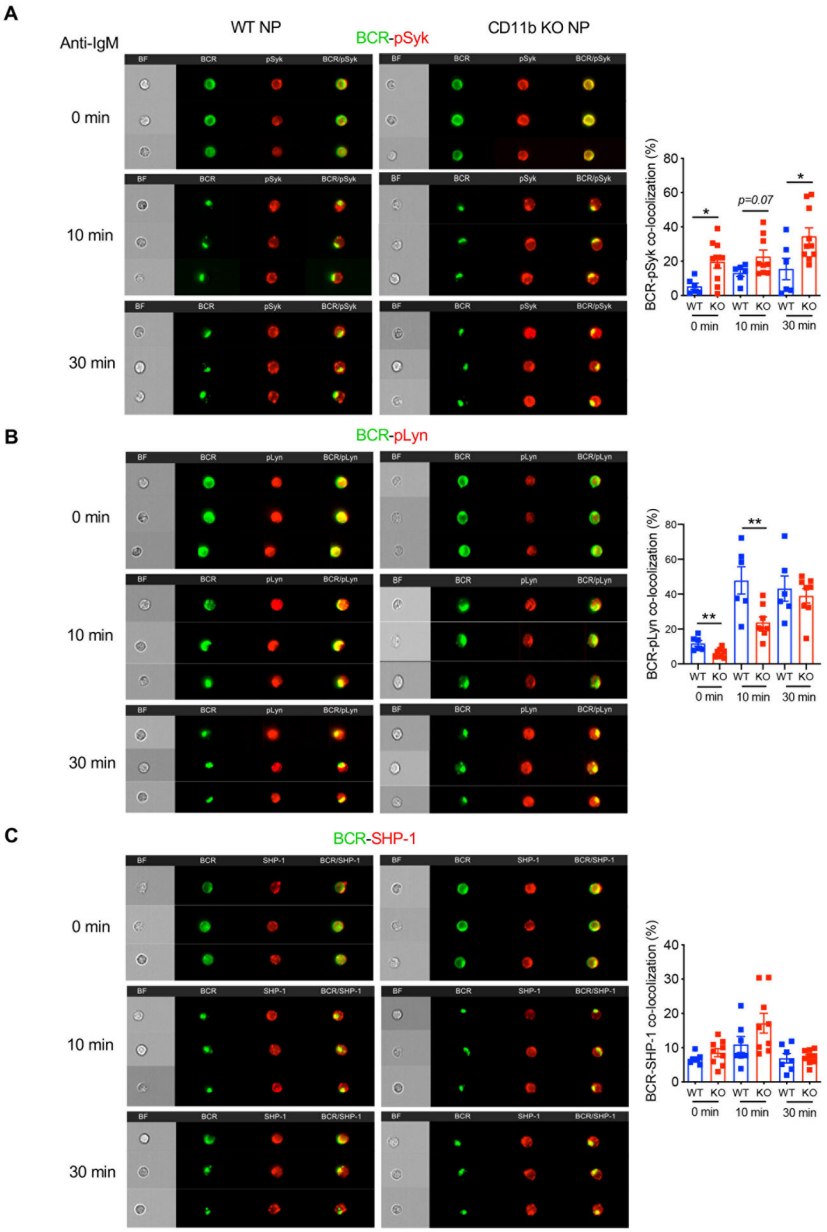

Figure 3. The loss of CD11b alters BCR signaling.

NP WT and NP CD11b KO mice were immunized by s.c. with a solution of 50 μg of NP-CGG emulsified in CFA at a 1:1 ratio. After 14 days, mice were boost immunized with 50 μg of NP-CGG in IFA at a 1:1 ratio. Draining LN cells at day 21 post-immunization were stimulated with 20μg/mL anti-IgM F(ab')2-FITC for given times and then stained with Abs against B220, phospho-Lyn, phospho-Syk, and SHP-1. B cell colocalization was measured via Imagestream, gated on $B220^+$ cells and defined by a similarity score. Representative images and summarized percentages of colocalized cells are shown. Each point represents an individual mouse sample. Data are shown as means ± s.e.m. *P<0.05; **P<0.01 (unpaired two-tailed Student's t-test). BF: bright field.

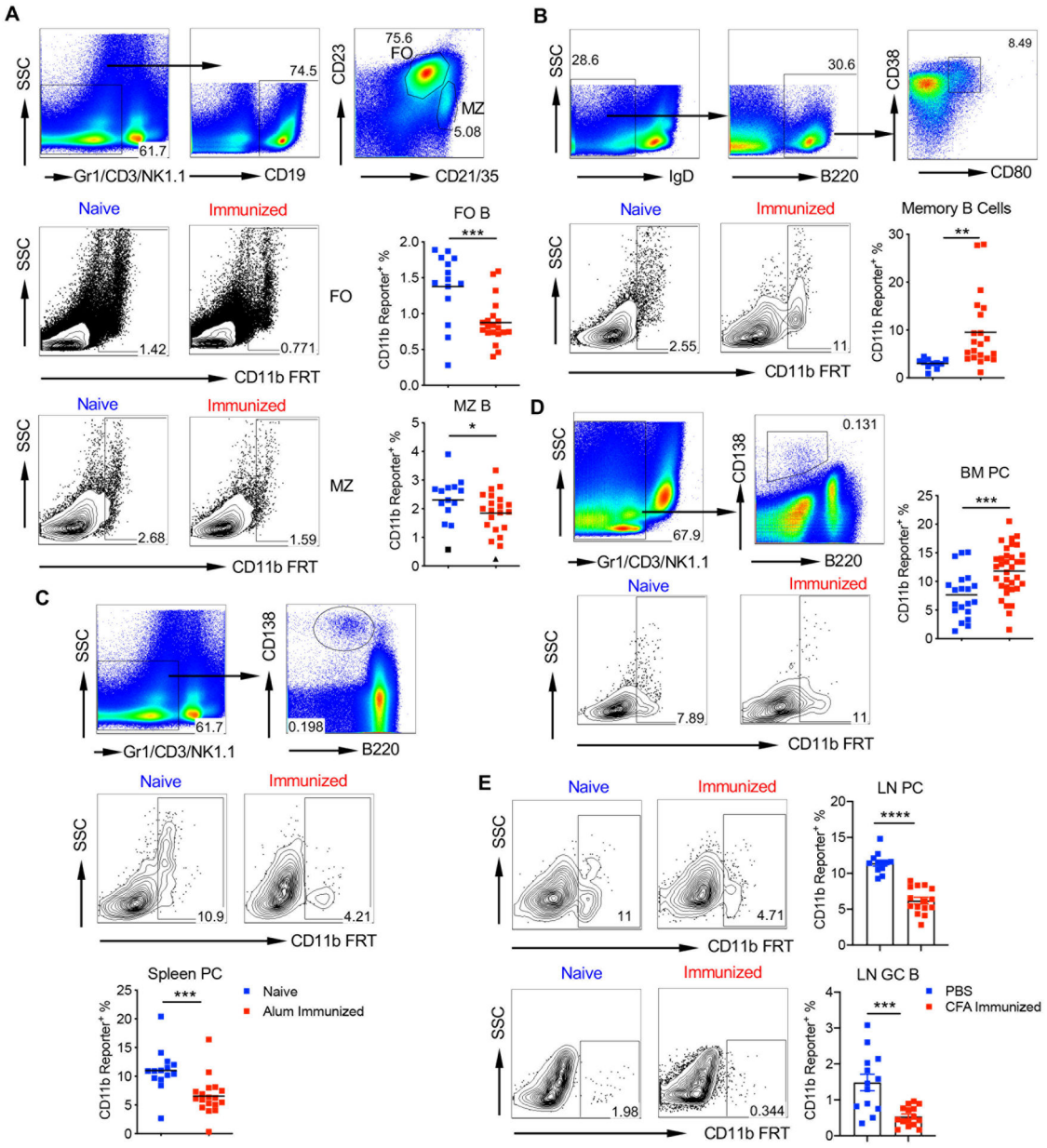

Figure 4. CD11b is dynamically expressed on different B cell subsets.

CD11b FRT reporter mice were immunized with 50μg of NP-CGG suspended in Alum via i.p. injection. Mice were sacrificed at day 14. Unimmunized mice (naïve) were used as controls. (A) CD11b expression on splenic FO and MZ B cells. Gating strategy, representative dot plots, and summarized data are shown. (B) CD11b expression on splenic memory B cells. Gating strategy, representative dot plots, and summarized data are shown. (C) CD11b expression on PCs. Gating strategy, representative dot plots, and summarized data are shown. (D) CD11b expression on PCs from BM. Gating strategy, representative dot plots, and summarized data are shown. (E) CD11b FRT reporter mice were immunized by s.c. injection with 100 μg of OVA or with the same volume of PBS in CFA at a 1:1 ratio and boosted with 100 μg of OVA in IFA after 14 days. Draining LNs were harvested on day

21 post-immunization. CD11b expression on PC or GC B cells is shown. Data are shown as means ± SEM. *P<0.05; **P<0.01; ***P<0.001; ****p < 0.0001 (unpaired two-tailed Student's t-test).

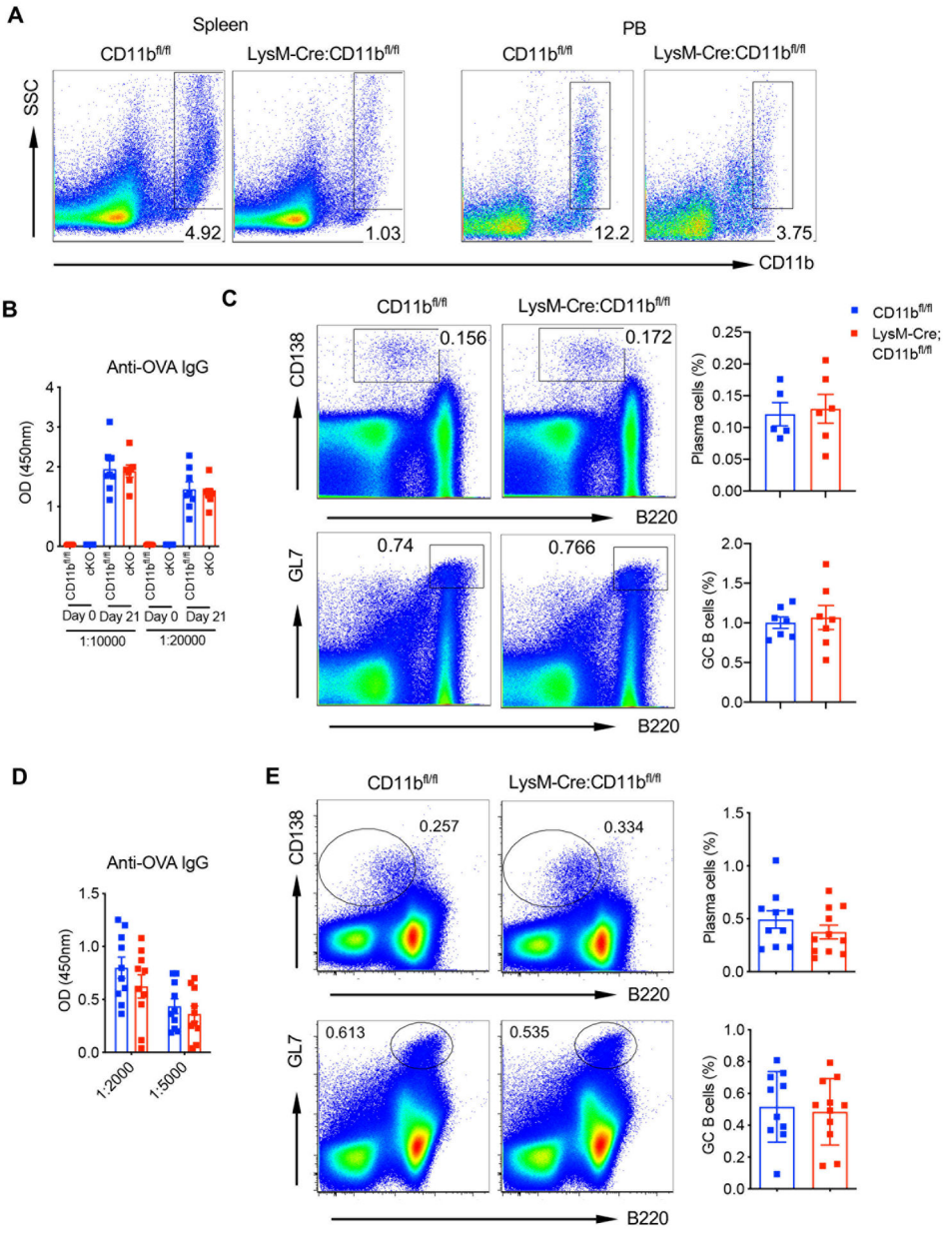

Figure 5. CD11b deficiency in myeloid cell does not impact the antibody response upon immunization.

(A) Efficiency of LyzM^{cre} driven deletion of CD11b. Spleen (left) and peripheral blood (PB) (right) from CD11b$^{fl/fl}$ and CD11$^{fl/fl}$LyzM$^{Cre/+}$ mice were stained with anti-CD11b Abs. Representative dot plots are shown. (B) CD11b$^{fl/fl}$ and CD11b$^{fl/fl}$LyzM$^{Cre/+}$ mice were immunized by s.c. injection with 100 μg of OVA in CFA and boosted with 100 μg of OVA in IFA after 14 days. Sera were collected before and at day 21 post-immunization. Anti-OVA IgG was measured via ELISA at given dilutions in plates coated with 1μg/well of OVA. (C) LNs were harvested on day 21 post-immunization. Representative FACS analysis of PCs and GC B cells and summarized data are shown. (D) CD11b$^{fl/fl}$ and CD11b$^{fl/fl}$LyzM$^{Cre/+}$ mice were immunized with 50μg of OVA suspended in Alum via i.p. injection. Sera were collected at day 14. Anti-OVA IgG was measured by ELISA. (E) Spleens from Alum

immunized mice at day 14 were stained for PC and GC B cells. Representative dot plots and summarized data are shown. Each dot represents one individual mouse sample.

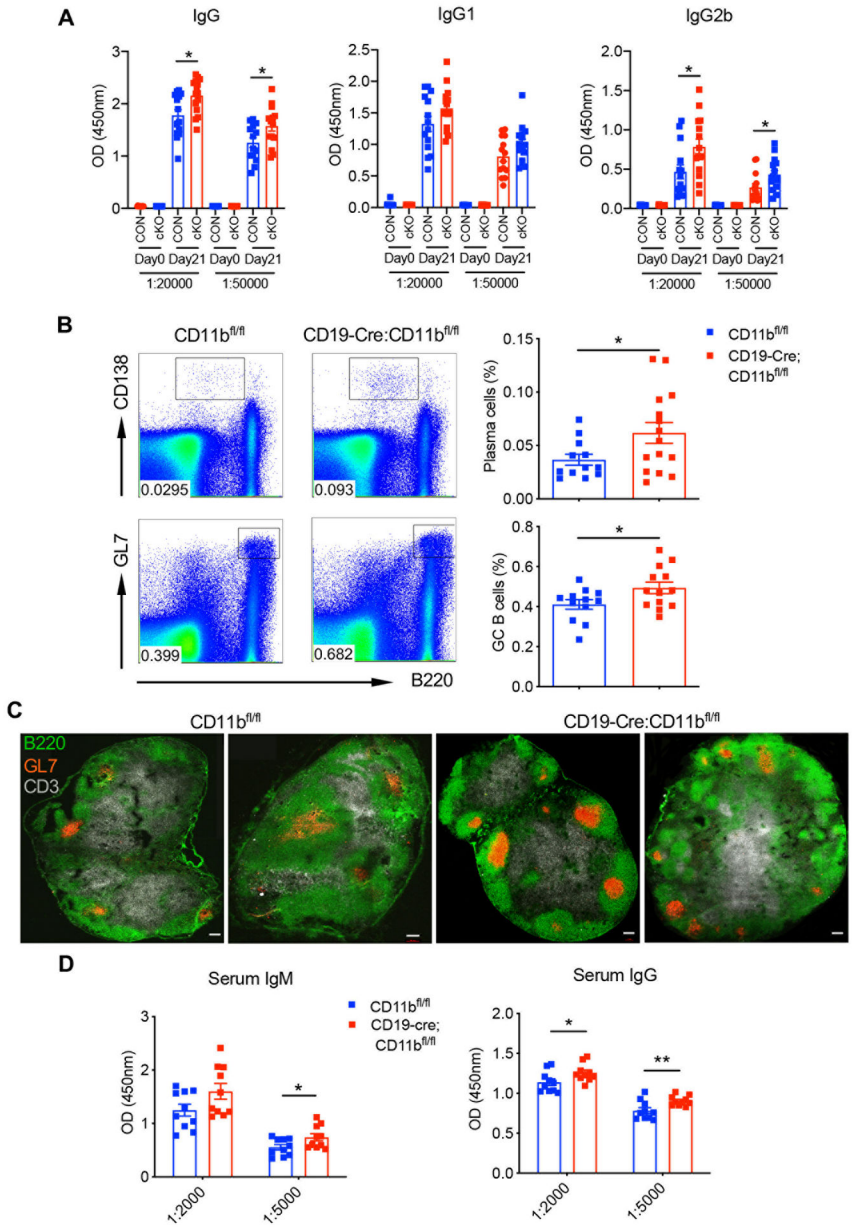

Figure 6. Loss of CD11b in B cells leads to increased serum antibody as well as PCs and GC formation.

$CD11b^{fl/fl}$ and $CD11b^{fl/fl}CD19^{Cre/+}$ mice were immunized by s.c. injection with 100 μg of OVA in CFA and boosted with 100 μg of OVA in IFA after 14 days. (A) Sera were collected before and at day 21 post-immunization. Anti-OVA IgG, IgG1, and IgG2b were measured by ELISA. (B) Draining LNs were harvested on day 21 post-immunization. FACS analysis of PCs and GC B cells was performed. Representative dot plots and summarized data are shown. (C) Draining LNs from control and cKO mice were snap frozen in the OCT medium and cryosectioned. Slides were then stained with antibodies against B220, GL7, and CD3. Scale bar: 100μm. (D) $CD11b^{fl/fl}$ and $CD11b^{fl/fl}CD19^{Cre/+}$ mice were immunized with 50μg of OVA suspended in Alum via i.p. injection. Sera were collected at day 14. Anti-OVA

IgG and IgM were measured by ELISA. *P<0.05; **P<0.01 (unpaired two- tailed Student's t-test).

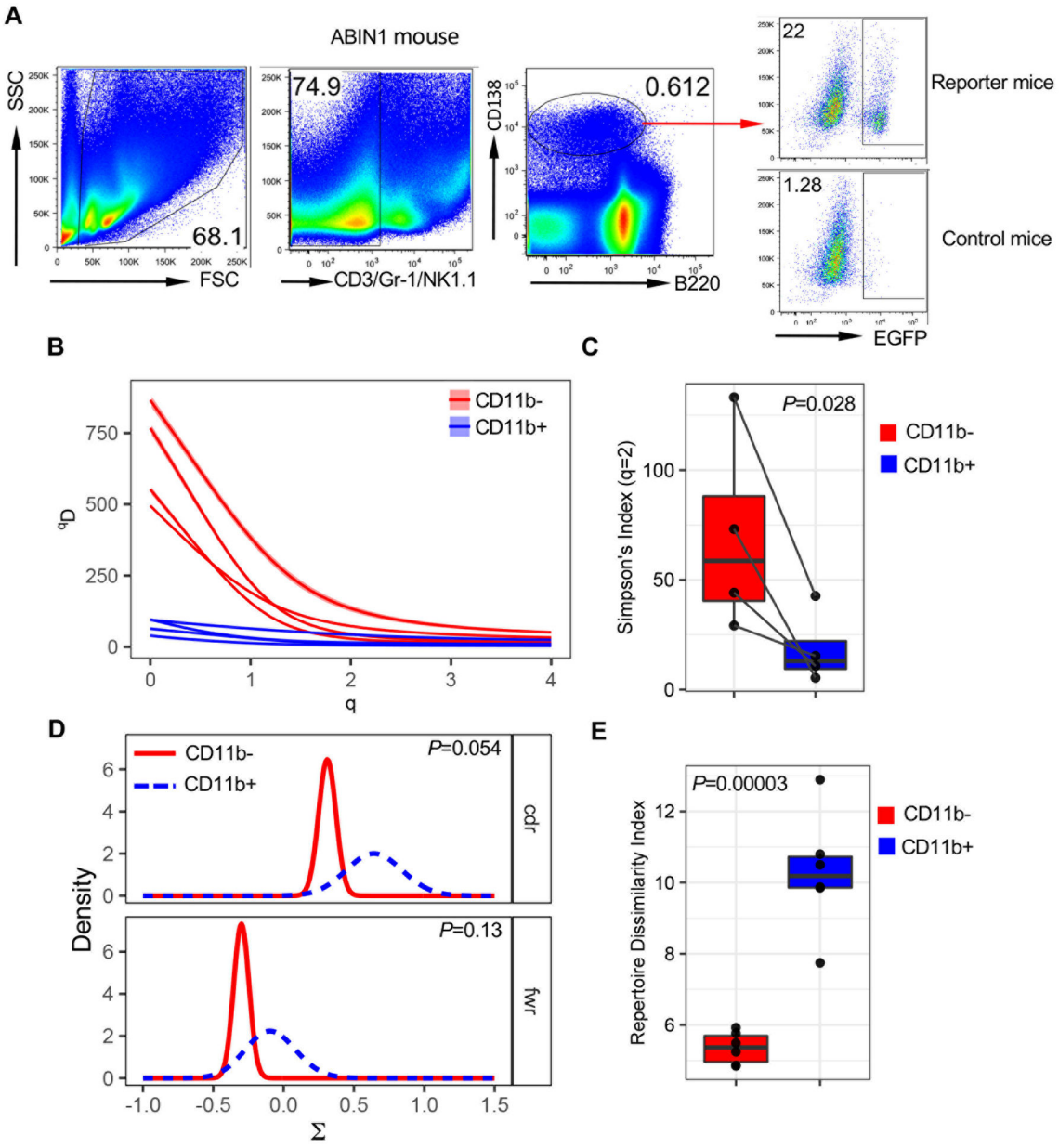

Figure 7. CD11b expression regulates Ab repertoire diversity, abundance, and selection.

(A) Gating strategy to sort CD11b+ versus CD11b- PCs from ABIN1[D485N] CD11b reporter mice (n=6). Dump gating (CD3/Gr-1/NK1.1) was used. CD11b+ vs CD11b- plasma cells were subjected to Repseq. (B) Antibody repertoire diversity curves for CD11b- (red) and CD11b+ (blue) PCs analyzed from four mice. The diversity metric (y axis) is plotted against diversity orders (q=0–4, x axis) for each sample. Shading around individual lines represents the 95% confidence intervals based on 200 bootstrap resamplings of reads from each repertoire. (C) Boxplot showing paired comparison of repertoire diversity estimated at q=2 (from panel B; representing the Simpson's Index) between CD11b- (red) and CD11b + (blue) PCs within the four mice analyzed (p value provided from one-tailed t-test). (D) Density plots representing evidence for selection strength (x axis) among clones present in

CD11b- (red) and CD11b+ (blue) PCs grouped across all four mice analyzed, split by CDR and FWR regions within the IGHV segment (p values provided represent a two-side test of differences between the posterior probability density function of each cell group). (E) Boxplot displaying RDI values for within group (CD11b−; CD11b+) comparisons based on IGHV repertoire-wide gene usage profiles (p value provided from one-way ANOVA).